

# Crack Formation and Shape of Fracture Surface in Tabular-Alumina-Based Castables with Addition of Specific Aggregates

J. Schnieder\*, L. Lynen, N. Traon, T. Tonnesen, R. Telle

RWTH Aachen University, Institute of Mineral Engineering, Templergraben 55, 52062 Aachen, Germany  
received November 08, 2013; received in revised form January 17, 2014; accepted March 13, 2014

## Abstract

Understanding the mechanical fracture and the microstructural behavior of refractories subject to thermal shock treatment is fundamental for the design of high-performance refractory materials. In recent decades, understanding has been focused on mechanisms occurring at the crack tip, namely in advanced ceramics. The focus recently switched to phenomena occurring in a different process zone of the crack, the wake region or following process zone. To understand the mechanisms in this wake region, specific aggregates are used in a model castable formulation based on tabular alumina, namely eutectic aggregates composed of  $\text{Al}_2\text{O}_3\text{-ZrO}_2\text{-SiO}_2$  and  $\text{Al}_2\text{O}_3\text{-ZrO}_2$ . The influence of these aggregates on the elastic and thermo-mechanical properties as well as on the crack path and the fracture surface is examined. This survey will put emphasis on the impact of each aggregate on the fracture surface and the crack path after the model castable has undergone several thermal shock cycles.

*Keywords:* Refractories, microstructure analysis, eutectic aggregates, thermal shock

## I. Introduction

Creating new surfaces is the first mechanism to consume energy in fracture mechanics. The energy for crack propagation is provided by the stored elastic energy. As far as refractories are concerned, in recent years the examination of the wake region behind the crack tip has been the focus of research activity. The well-known mechanisms like crack branching and crack deflection occur at the crack tip. But not only energy is consumed for creating new surfaces but also through other physical effects which are located behind the frontal process zone<sup>1</sup>. Different studies on rising R-curves point out the relevance of those mechanisms. The crack surface interaction in the wake region affects with increasing length the shielding effect at the crack tip. This results in an increase in macroscopic crack resistance and a rising R-curve<sup>2,3</sup>.

The strengthening behind the frontal process zone depends on different mechanisms. Different authors have defined them as friction between aggregate and matrix, crack bridging and bridging of liquid phases at higher temperatures. The effects related to aggregates depend on their size, shape and own properties<sup>4-6</sup>.

The effect of eutectic aggregates on the thermal shock resistance was recently examined<sup>7,8</sup>. Increased fracture energy and thermal shock resistance, calculated by  $R''''$ , was observed. Other authors have also examined the influence of eutectic aggregates ( $\text{Al}_2\text{O}_3\text{-ZrO}_2\text{-SiO}_2$ ) in order to investigate the special inner structure of those grains. The zirconia phase transformation (tetragonal – monoclinic) and the thermal expansion coefficient mismatch caused micro-cracks that interacted with cracks resulting from

thermal shock load. Observed transgranular and intergranular cracks resulted in pull-out effects as well as bridging mechanisms<sup>9,10</sup>. The use of andalusite, well known for its good thermal shock resistance, in a model system with glass showed interesting effects like debonding and microcrack generation depending on the thermal expansion mismatch. The anisotropic behavior of andalusite and also after mullite transformation at higher temperatures was made responsible for the effects described<sup>11,12</sup>.

## II. Experimental Procedure

As a reference castable, a standard LCC formulation was used. The castable was composed of 82.5 mass% tabular alumina aggregates, 12.5 mass% fine reactive alumina and 5 mass% calcium aluminate cement (Table 1). The sintered  $\text{Al}_2\text{O}_3$  raw material used was provided by Alteo and the cement by Kerneos. From the reference formulation, the granular fraction 2.24 – 3.0 mm of tabular alumina was separated by sieving, approximately 12.0 wt% of the mixture, and replaced with the same amount of eutectic aggregates  $\text{Al}_2\text{O}_3\text{-ZrO}_2\text{-SiO}_2$  (AZS) and  $\text{Al}_2\text{O}_3\text{-ZrO}_2$  (AZ) or andalusite (A). The AZS material was supplied by REFEL, the AZ by Alteo and the andalusite by DAMREC.

The samples were cast as prismatic bars with the following geometry: 160 mm · 40 mm · 40 mm. Each composition was cast after mixing and then cured for 48 h at room temperature in a humid environment and dried at 110 °C for 24 h. The samples were sintered for 6 h at 1500 °C with a heating and cooling rate of 2 K/min. The elastic properties were determined with a Resonant Frequency Damping Analyzer (RFDA) according to ASTM C 1548 – 02 (2012). The automatic impulse excitation measurement system was fabricated by IMCE. Modulus of Rupture (MOR)

\* Corresponding author: [schnieder@ghi.rwth-aachen.de](mailto:schnieder@ghi.rwth-aachen.de)

was measured with an Instron Universal Testing Machine after heat treatment and after 1,3,5,7 and 10 thermal shock cycles according to DIN EN 993–6. Three samples were measured for the thermal shock cycles and the averages are presented. The thermal shock tests were performed according to DIN EN 993–11 with quenching in air at a temperature of 850 °C.

**Table 1:** Formulation of the reference castable.

		Ref	A	AZ	AZS
		wt%	wt%	wt%	wt%
CA Cement	Secar71	5	5	5	5
Reactive Alumina	PFR	12.5	12.5	12.5	12.5
Tabular Alumina	0–0.045 mm	10	10	10	10
Tabular Alumina	0–0.3 mm	10	10	10	10
Tabular Alumina	0.2–0.6 mm	10	10	10	10
Tabular Alumina	0.5–1 mm	17.5	17.5	17.5	17.5
Functional	2.24–3.0 mm		11.8	12.3	11.7
Tabular Alumina	1–3 mm	35	23.2	22.7	23.3
	Total	100	100	100	100
Water	H <sub>2</sub> O	5	5	5	5
Deflocculant	FS40	0.15	0.15	0.15	0.15
Retarder	Citric acid	0.03	0.03	0.03	0.03

### III. Results and Discussion

This examination was conducted to get an impression of the mechanisms of crack formation and crack propagation after a defined thermal shock with different types of aggregates. The elastic properties and modulus of rupture, the fracture surfaces and polished micro sections were considered in the mentioned order.

As documented<sup>13</sup>, the use of functional aggregates reduced the modulus of rupture (MOR) and the Young's modulus after sintering because of microstructural effects.

Addition of A and AZ aggregates reduced the initial values of the Young's modulus. The tested formulation based on eutectic and andalusite aggregates showed the same trend of evolution of the Young's modulus after the different thermal shock cycles (Fig. 1). The reference castable exhibits a very high retained value of Young's modulus. After the strong impact of the first three thermal shock cycles with a decrease between 25 % and 54 %, the values dropped for the next seven thermal shock cycles only slightly by around 10–15 % (Table 2).

**Table 2:** Residual Young's modulus after 1, 3, 6, 10 thermal shocks.

Residual Young's modulus in [%]				
	1.TS	3. TS	6. TS	10. TS
A	63.9	46.1	35.7	29.3
AZ	74.0	57.2	45.8	39.1
AZS	78.5	60.5	53.5	45.8
Ref	90.9	78.6	75.1	67.5

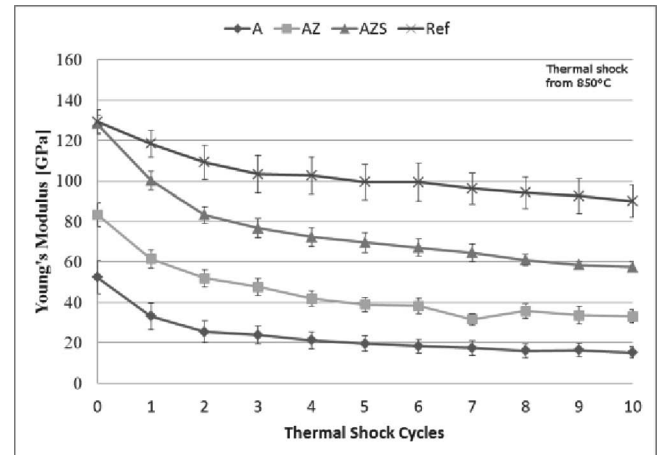


**Fig. 1:** Evolution of Young's modulus after different thermal shock cycles.

For the modulus of rupture (Fig. 2) results, two groups of castables could be distinguished: castables AZ and A exhibit the highest values after the whole series of thermal shock cycles. AZS and Ref exhibited very high initial values with a considerable depletion of mechanical strength after ten thermal shock cycles. As for the Young's modulus, all castables showed a strong depletion during the first three thermal shock cycles. Afterwards, the values of the modulus of rupture remained almost on the same constant level. The slight increase of the values after some thermal shocks could be explained by statistical deviation from samples.

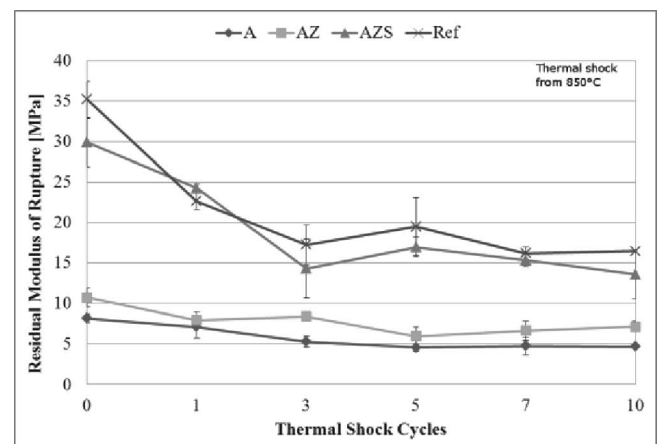


**Fig. 2:** Residual Modulus of Rupture after different thermal shock cycles.

The fracture surfaces after the three-point bending test showed interesting features. The castable with andalusite aggregates transformed into mullite (Fig. 3), revealed a brittle transgranular fracture with large cracks between the aggregates and the matrix as well as small cracks inside the aggregates. In contrast to this, the AZ aggregates remain in their original shape, as shown in Fig. 4. Debonding between aggregate and matrix was observed for most of the samples regardless of the count of thermal cycles, even after firing. Friction between the aggregates and the matrix is a possible phenomenon. The samples were still coherent even after catastrophic failure.

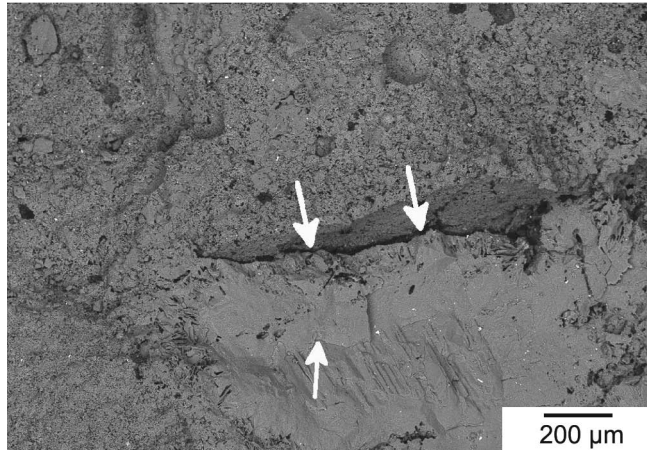


Fig. 3 : Castable A after 1 thermal shock cycle (fracture surface).

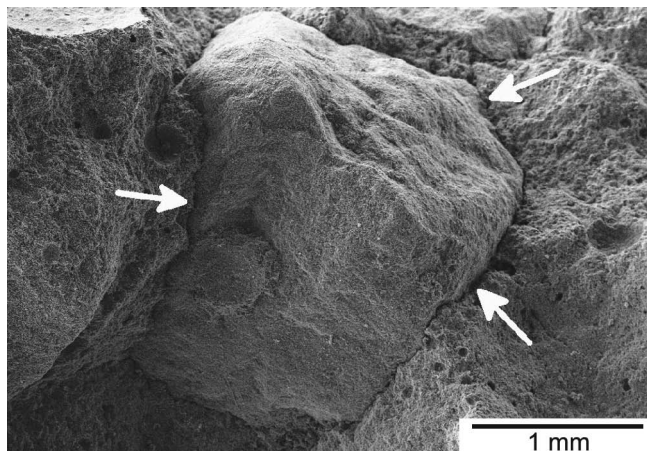


Fig. 4 : Castable AZ after 1 thermal shock cycle (fracture surface).

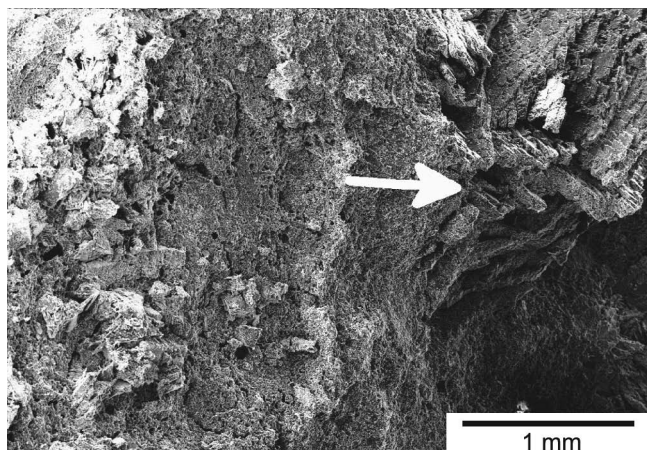


Fig. 5 : Castable AZS after 1 thermal shock cycle (fracture surface).

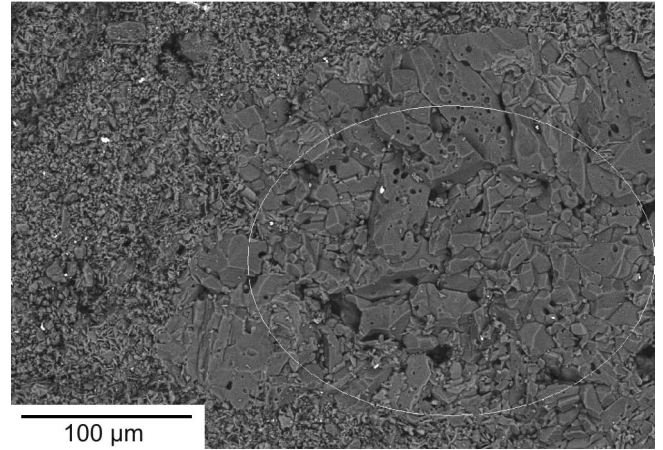


Fig. 6 : Castable Ref after 1 thermal shock cycle (fracture surface).

Fig. 5 represents the fracture surface of a AZS sample after the bending strength test. The back-scattered detection picture on the left side (Fig. 5) showed a brittle fracture surface. The amorphous SiO<sub>2</sub> phase left the aggregate, leaving a very porous grain after sintering. The rough surface is clearly seen in Fig. 6.

The polycrystalline tabular alumina grain showed a brittle fracture surface, as shown in Fig. 6. No debonding was observed between aggregates and matrix.

In case of andalusite-based castables, the matrix and the aggregates showed a considerable density of progressively propagating trans- and intergranular cracks. During sintering the andalusite transformed almost completely into mullite associated with the irreversible expansion above 1280 °C<sup>11,12</sup>. This transformation and the thermal shock experiments induced a dense microcrack network inside the aggregates (Fig. 7). Large cracks also expand from the center to the grain boundaries. At these boundaries, the grain partially debonded from the matrix. This debonding and the number of cracks are responsible for the low elastic and mechanical properties.

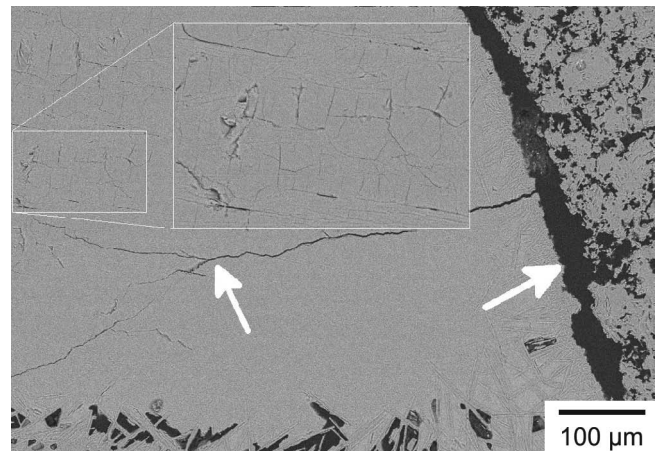


Fig. 7 : Castable A microstructure after 10 thermal shocks.

In addition to this, a needle-like-shaped structure was developed at the interface between aggregate and matrix (Fig. 8). Those needles were constituted mainly of alumina. Some cracks were also deflected by needles embedded in the mullite aggregate.

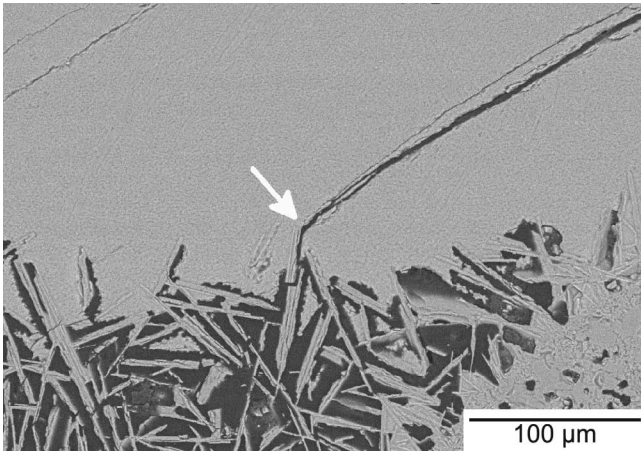


Fig. 8 : Castable A after 5 thermal shocks.

AZ-based castables showed a lesser dense crack network than in andalusite sample. After firing, debonding of the AZ and some severe microcracking within the tabular alumina aggregates were observed (Fig. 9), resulting in low elastic properties and strength values.

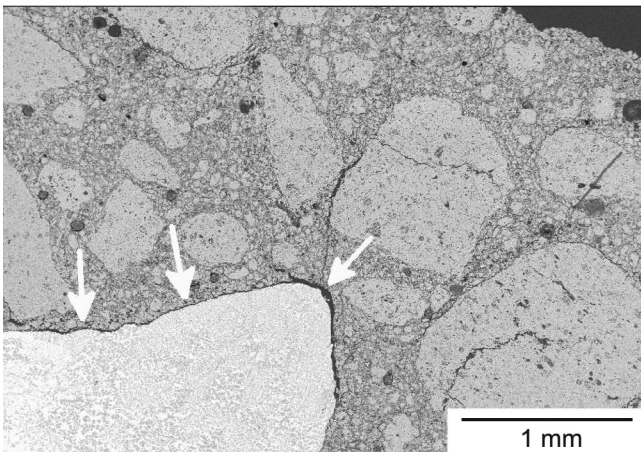


Fig. 9 : Overview of AZ after firing.

After one thermal shock, some AZ aggregates exhibited some severe internal cracking (Fig. 10) caused by the phase transformation of  $ZrO_2$  during firing or by the first thermal shock cycle. This effect was, however, not observed in all samples. Indeed, even after ten thermal shock cycles, some aggregates did not show any crack formation.

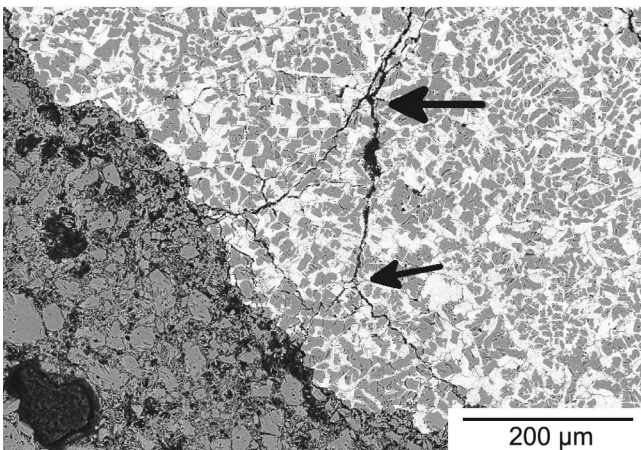


Fig. 10 : Castable AZ after 1 thermal shock cycle.

The amorphous  $SiO_2$  of the eutectic AZS aggregates reacted during sintering with the alumina and calcium aluminate phases of the matrix leading to the formation of a very porous microstructure (Fig. 11). Microcracking in the  $Al_2O_3$  matrix of the aggregate appeared after transformation of the  $ZrO_2$  phase during sintering. The porous aggregates acted as structural elements preventing crack propagation. Strong stresses induced severe cracking inside the aggregates after ten thermal shock cycles.

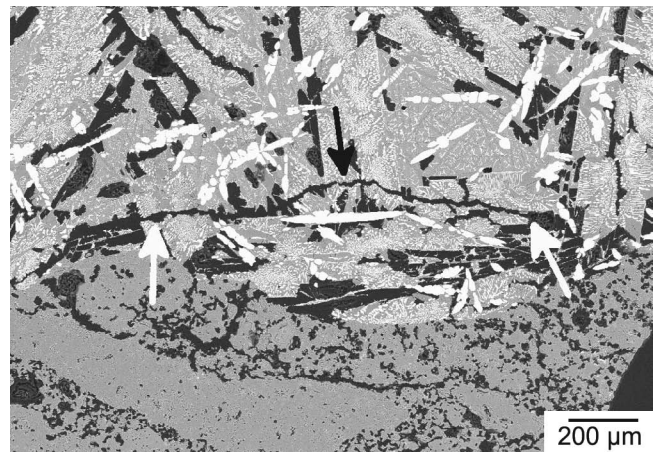


Fig. 11 : Castable AZS aggregate after 10 thermal shock cycles.

Large isolated cracks can also be observed within the microstructure of AZS sample (Fig. 12). These cracks are intergranular in sections with small grains and transgranular in sections with large grains. Transgranular crack formation could only be detected after ten thermal shock cycles. The microstructure after sintering was free of cracks.

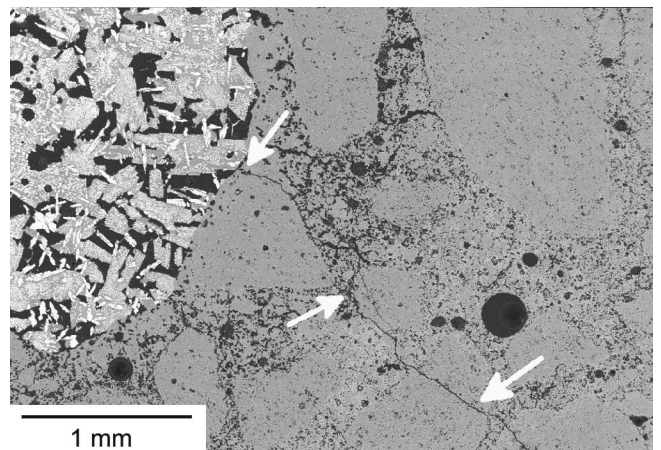


Fig. 12 : Overview of AZS after 10 thermal shocks.

The reference castable (Ref), as shown in Fig. 13, exhibited almost no damage after the first thermal shock. With increased number of cycles some damage occurred in the microstructure, notably intergranular cracks propagating along alumina aggregates and cracks inside the aggregates (Fig. 14). The low crack density in the microstructure of the castable can explain the high retained Young's modulus after ten thermal shocks.

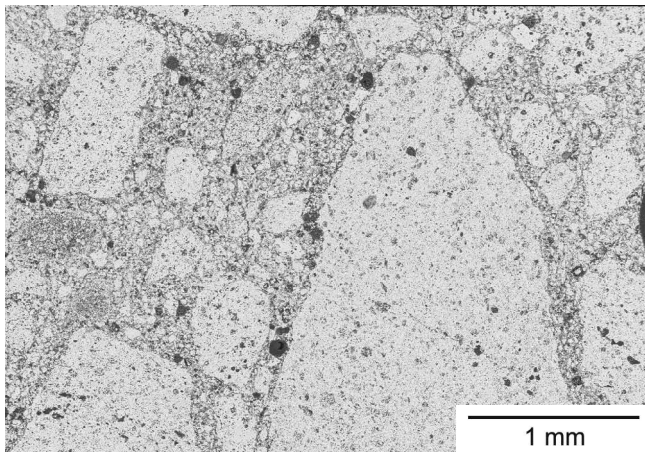


Fig. 13: Overview Ref after 3 thermal shocks.

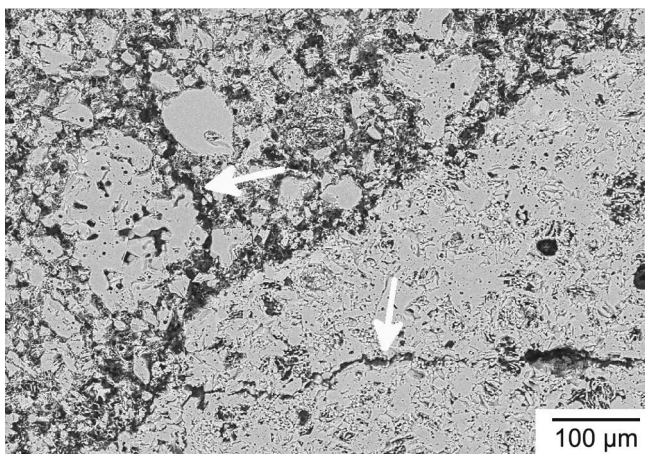


Fig. 14: Cracks in Ref after 10 thermal shocks.

#### IV. Conclusions

The addition of eutectic and andalusite aggregates with a grain size of 2.24–3.00 mm had a strong impact on the elastic and thermo-mechanical properties of high-alumina castables. The following aspects could be evaluated:

All four castables showed the same trend of stiffness evolution after each thermal shock cycle. The values of the retained Young's modulus for the Ref castable were distinctly higher than those of the formulations with eutectic and andalusite aggregate addition. Two groups of materials could be distinguished: Ref + AZS with a drastic decrease of toughness from a very high initial value. The A + AZ formulation started with a low initial modulus of rupture value but the depletion was not so strong after the thermal shock cycles<sup>13</sup>.

The addition of A resulted in mullite aggregate formation after sintering. The grain developed at parts of the grain boundaries a transition zone of pores and needle-like structures. With increasing number of thermal shock cycles the damage inside the grains and the matrix became more severe and is responsible for the low residual values of Young's modulus (around 30 % for A and 40 % AZ). AZ aggregates resulted also in a strong decrease of the Young's modulus. The debonding caused by the thermal expansion mismatch could also explain the low mechanical and elastic values for this formulation. The thermal shocks and the crack generation combined with pre-

formed cracks after sintering resulted in pull-out effects. The high retained strength after several thermal shock cycles was an effect of the lower amount of stored elastic energy which is proportional to  $\sigma^2/E$ <sup>1</sup>.

The tested Ref and AZS showed the same toughness and stiffness after sintering. After three-point bending tests, both castables showed a brittle fracture surface. The rough surface of the AZS aggregates was induced through the porous structure after the amorphous SiO<sub>2</sub> infiltrated the matrix during sintering. The distribution of the pores inside the aggregates is random and therefore the fracture area, too. The crack path changed with increased number of thermal shock cycles from intergranular cracks to a combination of inter- and transgranular cracks. This corresponded to the around 55 % lower values for the elastic modulus and strength.

For further explanations, the focus will be on the crack bridging and friction between aggregates and matrix and their effect on R-curves. The fracture energy is also an important parameter for better understanding of the energy consumption by the different mechanisms. The extension of Hasselman's thermal shock theory<sup>14,15</sup> showed clearly the influence of crack interaction in the microstructure, fracture energy and R-curves. In addition to the use of aggregates of different nature, the impact of the exchange of aggregates of the granular fractions 0.2–0.6 mm will be examined. Finally, the thermal shock test results will be compared with a new high temperature thermal shock test where the samples are shocked between two high temperatures (e.g. between 1600 °C and 750 °C) with the same  $\Delta T$ .

#### Acknowledgements

The authors would like to express their thanks to the German Research Foundation. This project is supported in the framework of the priority program 1418 "Microstructural processes in the wake region of the crack in castables containing eutectic aggregates at high temperature thermal shock".

The authors are also grateful to Alteo, Kerneos, DAM-REC, REFEL and BASF for supporting this work with raw materials.

#### References

- 1 Refractories handbook, edited by Charles A. Schacht, Chapter 2, Bradt, R.C., Fracture of Refractories, 11–38, ISBN: 0–8247–5654–1
- 2 Steinbrech, R.W., Reichl, A., Schaarwächter, W.: R-curve behavior of long cracks in alumina, *J. Am. Ceram. Soc.*, **73**, [7], 2009–2015, (1990).
- 3 Steinbrech, R.W., Schmenkel, O.: Crack resistance curves of surface cracks in alumina, *J. Am. Ceram. Soc.*, **71**, [5], C-271–273, (1988).
- 4 Skiera, E., Malzbender, J., Mönch, J., Dudczig, S., Aneziris, C.G., Steinbrech, R.W.: Controlled crack propagation experiments with a novel alumina-based refractory, *Adv. Eng. Mater.*, **14**, [4], 248–254, (2012).
- 5 Bradt, R.C.: Crack extension in refractories. Proc. Unitecr '11; Kyoto 30.10.-02.11.(2011), Paper No. 2-D-5
- 6 Harmuth, H., Bradt, R.C.: Investigation of refractory brittleness by fracture mechanical and fractographic methods, *Refractories Manual*, 6–10, (2010).

- 7 Miyaji, D.J., Tonnesen, T., Rodrigues, J.D.A.: Eutectic aggregates containing refractory castables: What are their effects on fracture energy and thermal shock damage resistance? Proc. Unitecr '11, Kyoto, 30.10.-02.11.2011, Paper No. 2-D-3.
- 8 Miyaji, D.J., Otofujii, C., Rodrigues, J.D.A.: The load-displacement curve of steady crack propagation: An interesting source of information for predicting the thermal shock damage of refractories Proc. Unitecr '13, Victoria, Paper No. 17–10.
- 9 Pandolfelli, V.C., Salvini, V.R., Brant, P.O.R.C., Noronha, R.T.T., Mattos, U.: Influence of mullite-zirconia aggregate addition on the thermomechanical properties of high-alumina refractories, Unitecr '93 Congress, Sao Paulo, Brazil, 1993.
- 10 Pandolfelli, V.C., Salvini, V.R., Rodrigues, J.A., Hübner, H., Wolf, C.: Evaluation of thermomechanical properties of alumina refractories containing a fused mullite-zirconia aggregate, Unitecr '95, Kyoto, Japan, 2, 1995.
- 11 Tessier-Doyen, N., Glandus, J.C., Huger, M.: Anisotropic untypical Young's modulus evolution of model refractories at high temperature, *J. Eur. Ceram. Soc.*, **26**, 289–295, (2006).
- 12 Kakroudi, M.G., Huger, M., Gault, C., Chotard, T.: Anisotropic behaviour of andalusite particles used as aggregates on refractory castables, *J. Eur. Ceram. Soc.*, **29**, 571–579, (2009).
- 13 Schnieder, J., Lynen, L., Traon, N., Tonnesen, T., Telle, R.: Influence of eutectic aggregates in castables on the thermal shock resistance, International Colloquium on Refractories 2013, Aachen.
- 14 Hasselmann, D.P.H.: Unified theory of thermal shock fracture initiation and crack propagation in brittle ceramics, *J. Am. Ceram. Soc.*, **52**, [11], 600–604, (1969).
- 15 Salvini, V.R., Pandolfelli, V.C., Bradt, R.C.: Extension of hasselman's thermal shock theory for crack/microstructure interaction in refractories. *Ceram. Int.*, **38**, 5369–5375, (2012).